J Comput Aided Mol Des (2011) 25:1019–1032
DOI 10.1007/s10822-011-9481-6

Conformational studies of immunodominant myelin basic protein 1–11 analogues using NMR and molecular modeling

Despina Laimou · Eliada Lazoura · Anastassios N. Troganis · Minos-Timotheos Matsoukas · Spyros N. Deraos · Maria Katsara · John Matsoukas · Vasso Apostolopoulos · Theodore V. Tselios

Received: 19 May 2011 / Accepted: 17 October 2011 / Published online: 1 November 2011

Abstract Two dimensional nuclear magnetic resonance studies complimented by molecular dynamics simulations were conducted to investigate the conformation of the immunodominant epitope of acetylated myelin basic protein residues 1–11 (Ac-$MBP_{1–11}$) and its altered peptide ligands, mutated at position 4 to an alanine (Ac-$MBP_{1–11}$[4A]) or a tyrosine residue (Ac-$MBP_{1–11}$[4Y]). Conformational analysis of the three analogues indicated that they adopt an extended conformation in DMSO solution as no long distance NOE connectivities were observed and seem to have a similar conformation when bound to the active site of the major histocompatibility complex (MHC II). The interaction of each peptide with MHC class II I–A^u was further investigated in order to explore the molecular mechanism of experimental autoimmune encephalomyelitis induction/inhibition in mice. The present findings indicate that the Gln^3 residue, which serves as a T-cell receptor (TCR) contact site in the TCR/peptide/I–A^u complex, has a different orientation in the mutated analogues especially in the Ac-$MBP_{1–11}$[4A] peptide. In particular the side chain of Gln^3 is not solvent exposed as for the native Ac-$MBP_{1–11}$ and it is not available for interaction with the TCR.

Keywords Experimental autoimmune encephalomyelitis · Multiple sclerosis · Central nervous system · Myelin basic protein · Major histocompatibility complex class II · T-cell receptor

Introduction

Multiple sclerosis (MS), is an autoimmune disease characterized by a coordinated inflammatory attack resulting in the destruction of myelin sheath in the central nervous system (CNS) leading to body paralysis [1, 2]. It is widely considered that $CD4^+$ T helper type 1 (Th1) cells play a pivotal role in mediating an autoimmune attack against components of myelin sheath [3]. Additional cells, such as $CD8^+$ T cells, macrophages, complement and more recently Th17 cells are also involved in axonal damage and neurodegeneration. Experimental autoimmune encephalomyelitis (EAE), an animal model of MS has many characteristics of MS, and is used to assess the efficacy of vaccine and immunotherapeutic peptide candidates derived from myelin basic protein (MBP), proteolipid protein (PLP) and myelin oligodendrocyte glycoprotein (MOG) [4, 5]. One of the immunodominant encephalitogenic epitopes of MBP which induce EAE, is the acetylated N-terminal 11-mer peptide, Ac-$MBP_{1–11}$ (AcASQKRPSQRHG), or the shorter Ac-$MBP_{1–9}$ [6–9]. Interestingly, the symptoms of EAE are rarely observed using the intermediate mutant peptide analogue, with one amino acid mutation at position 4 of Ac-$MBP_{1–9}$ peptide, with Ala, and not at all with Tyr [10]. The Ac-$MBP_{1–11}$[4A] analogue totally inhibits the EAE symptoms induced by encephalitogenic

Despina Laimou and Eliada Lazoura contributed equally to this work.

D. Laimou · M.-T. Matsoukas · S. N. Deraos · M. Katsara · J. Matsoukas · T. V. Tselios (✉)
Department of Chemistry, University of Patras, 26500 Patras, Greece
e-mail: ttselios@upatras.gr

E. Lazoura · M. Katsara · V. Apostolopoulos
Centre for Immunology, Burnet Institute, Melbourne, VIC 3004, Australia

A. N. Troganis
Department of Biological Applications and Technologies, University of Ioannina, 45110 Ioannina, Greece

Ac-$MBP_{1–11}$ epitope when co-injected in (PL/J x SJL)F1 mice [9]. These results imply that Ac-$MBP_{1–11}$[4A]-induced immunomodulation that inhibits EAE in vivo.

Furthermore, studies have indicated that the residue at position 4 in $MBP_{1–11}$ peptide plays a pivotal role in binding of the peptide to MHC class II, I–A^u [11, 12]. In particular, the mutated analogue, Ac-$MBP_{1–11}$[4A] binds to I–A^u with at least a 50-fold higher affinity compared to the native Ac-$MBP_{1–11}$ peptide [9, 13]. Moreover, the mutation at position 4 of Lys to Tyr (Ac-$MBP_{1–11}$[4Y]) enhances the stability of the I–A^u-peptide complex, having a 1500-fold higher affinity, which stimulates Ac-$MBP_{1–11}$ T cells more effectively compared to Ac-$MBP_{1–11}$[4A] [13, 14]. However, the 9-mer or 11-mer $MBP_{1–11}$ peptides dissociates rapidly, when complexed with I–A^u or I–A^k [15]. The very short half-life of wild-type Ac-$MBP_{1–11}$ bound to I–A^u indicates a short life time in the thymus and an ineffective deletion of autoreactive T cells [16]. The addition of six amino acids from the $OVA_{323–328}$ peptide to the N-terminus of the $MBP_{1–9}$ epitope and mutation of Lys to Tyr at position 4 have resulted in increased binding affinity to I–A^u [11]. Molecular models of OVA-$MBP_{1–9}$ and OVA-$MBP_{1–9}$[4Y] peptides in complex with I–A^u, have indicated that the large aromatic phenyl group of Tyr^4 is predominantly buried into the P6 hydrophobic pocket within the I–A^u peptide binding groove [11].

The crystal structure of $MBP_{1–11}$[4Y] in complex with I–A^u (pdb code 1K2D), demonstrates that the MBP peptide sat in an unusual shifted register in the MHC groove, resulting in the P1 and P2 pockets devoid of peptide side chain and being occupied by several specifically ordered water molecules [12]. The large hydrophobic P6 pocket is accommodated by the aromatic ring of Tyr at position 4. Other significant studies have shown that glutamine (Gln) at position 3 and proline (Pro) at position 6 are solvent exposed and in contact with the T cell receptor (TCR) [12], hereas, the amino acid at position 4 and arginine (Arg) at position 5 bind to MHC. In addition, the structure of the 172.10 TCR in complex with I-A^u-$MBP_{1–11}$ have been analyzed to address and explain the immunological findings [17, 18].

To further understand the conformation of such biologically active peptides, Ac$MBP_{1–11}$, Ac$MBP_{1–11}$[4A] and Ac-$MBP_{1–11}$[4Y] Table 1, 2D NMR experiments were performed using dimethyl sulfoxide (DMSO) as solvent. Moreover, a theoretically comparative conformational analysis of Ac$MBP_{1–11}$, Ac$MBP_{1–11}$[4A] and Ac-$MBP_{1–11}$[4Y] peptides in complex with the X-ray structure of I–A^u (pdb code 1K2D) [12] was undertaken. The conformational characteristics of the peptides were explored in an attempt to correlate their EAE biological activity with the adopted conformation and to provide important structural characteristics for EAE antagonism. It is known that linear peptides on their own are sensitive to proteolytic degradation and they are not used in vivo, unless they are conjugated to a carrier or designed to be more stable. Thus, the de novo design of a stable molecule that will mimic the corresponding peptide, i.e. cyclic peptide or non-peptide mimetic, is pivotal in Medicinal Chemistry. A detailed conformational analysis of bioactive peptides using a combination of advanced 2D NMR and Molecular Modeling techniques are cornerstones in the rational drug design of non-peptide mimetics.

Results

NMR characterization of Ac-$MBP_{1–11}$, Ac-$MBP_{1–11}$[4A] and Ac-$MBP_{1–11}$[4Y] analogues in DMSO-d_6 solution

NMR techniques have been widely used to determine the presence of conformers with distinguishable populations in linear or cyclic peptides, peptide fragments derived from protein sequence and peptides of de novo design, even small and especially linear peptides in solution which are difficult due to their flexibility [19–21]. Such studies typically require the use of 2D correlation spectroscopy, usually TOCSY and NOESY experiments. Herein, TOCSY and NOESY experiments were performed for resonance assignment of the protons, the identification of the amino acid sequencing and the establishment of the NOE connectivities. The results of the chemical shifts for the studied analogues are reported in Table 2. The proton chemical shifts of Ac-$MBP_{1–11}$, Ac-$MBP_{1–11}$[4A] and Ac-$MBP_{1–11}$[4Y] analogues were almost identical, indicating the similarity of their backbone structures in DMSO-d_6 solution. The observed inter-residue cross-peaks in the NOESY spectrum and their intensities for Ac-$MBP_{1–11}$[4A] are reported in Table 3.

The proton chemical shifts of Ac-$MBP_{1–11}$, Ac-$MBP_{1–11}$[4A] and Ac-$MBP_{1–11}$[4Y] in the 1D ^1H NMR spectrum (Fig. 1) were assigned using 2D H^1–H^1 TOCSY and NOESY experiments. Additional information was then taken from the NOESY spectrum, in which sequential cross-peaks occurred between $C_\alpha H_i$ and NH_{i+1} resonances ($d_\alpha N_{(i,i+1)}$). The cross peak between the $C_\alpha H$ of the residue preceeding the proline and the $C_\delta H$ of the proline, was used to establish sequential assignment. This procedure allowed for the establishment of sequential backbone connectivities for the entire peptide and specific assignment of all resonances, as summarized in Table 2.

As with most short linear peptides in solution, the molecule is expected to be fluctuating over an ensemble of conformations with their φ and ψ angles lying within the broad minima of the conformational energy diagram [22].

Table 1 Primary structure of $MBP_{1–11}$ epitope and of the synthesized Ac-$MBP_{1–11}$, Ac-$MBP_{1–11}$[4A] and Ac-$MBP_{1–11}$[4Y] analogues

Name	Amino acid sequence										
	1	2	3	4	5	6	7	8	9	10	11
$MBP_{1–11}$	Ala	Ser	Gln	Lys	Arg	Pro	Ser	Gln	Arg	His	Gly
Ac $MBP_{1–11}$	Ac-Ala	–	–	–	–	–	–	–	–	–	–
Ac $MBP_{1–11}$ [4A]	Ac-Ala	–	–	Ala	–	–	–	–	–	–	–
Ac $MBP_{1–11}$ [4Y]	Ac-Ala	–	–	Tyr	–	–	–	–	–	–	–

Table 2 ^{1}H chemical shifts (ppm) of the residues in Ac-$MBP_{1–11}$ (normal), Ac-$MBP_{1–11}$[4A] (italics) and Ac-$MBP_{1–11}$[4Y] (bold) analogues at 298 K in DMSO-d_6 solution

	Residue	NH	αH	βH	Others
1	Ac-Ala	8.16	4.25	1.20	Ac:1.85
		8.13	*4.27*	*1.19*	*Ac:1.84*
		8.14	**4.27**	**1.19**	**Ac:1.85**
2	Ser	7.94	4.22	3.63; 3.57	
		7.94	*4.23*	*3.63*; *3.55*	
		7.93	**4.23**	**3.63**; **3.55**	
3	Gln	7.92	4.22	1.90; 1.72	γH:2.10, NH:7.29;6.82
		7.91	*4.22*	*1.71*	*γH:2.10*, *NH:7.28;6.80*
		7.96	**4.17**	**1.84**; **1.64**	**γH:2.06**, **NH:7.25;6.82**
4	Lys	7.92	4.22	1.62	γH:1.29, δH: 1.49, ε: 2.74, ζNH:7.68
	Ala	*7.96*	*4.24*	*1.17*	**2,6H:6.62**; **3,5H:6.99**
	Tyr	**7.89**	**4.41**	**2.85**; **2.63**	
5	Arg	8.00	4.47	1.69	γH:1.52, δH: 3.09, εNH:7.55
		8.02	*4.48*	*1.69*	*γH:1.52*, *δH: 3.09*, *εNH:7.50*
		8.11	**4.41**	**1.68**	**γH:1.51**, **δH: 3.07**, **εNH:7.47**
6	Pro	–	4.36	2.06	γH:1.85, δH:3.64;3.52
		–	*4.35*	*2.07*	*γH:1.85*, *δH 3.63;3.53*
		–	**4.35**	**2.06**	**γH:1.85**, **δH:3.50**
7	Ser	8.04	4.23	3.62; 3.57	
		8.05	*4.21*	*3.64*; *3.57*	
		8.04	**4.23**	**3.63**; **3.57**	
8	Gln	7.90	4.26	1.90; 1.72	γH:2.11, NH:7.30;6.88
		7.88	*4.25*	*1.74*	*γH:2.11*, *NH:7.32;6.89*
		7.88	**4.25**	**1.90**; **1.73**	**γH:2.11**, **NH:7.32;6.89**
9	Arg	8.08	4.23	1.65	γH:1.47, δH:3.06, εNH:7.51
		8.03	*4.21*	*1.65*	*γH:1.50*, *δH:3.06*, *εNH:7.51*
		8.03	**4.22**	**1.64**	**γH:1.47**, **δH:3.06**, **εNH:7.49**
10	His	8.28	4.62	3.10; 2.96	2H:8.93, 4H:7.35
		8.26	*4.62*	*3.10*; *2.96*	*2H:8.94*, *4H:7.35*
		8.27	**4.62**	**3.10**; **2.94**	**2H:8.95**, **4H:7.36**
11	Gly	8.33	3.81; 3.75		
		8.32	*3.81*; *3.75*		
		8.32	**3.81**; **3.75**		

Indeed, observation of extended regions of both sequential NOE connectivities $d_{\alpha N(i,i+1)}$ and $d_{NN(i,i+1)}$, indicated a conformational averaging between the a_R and b regions of φ, ψ space [23]. Specifically, $d_{NN(i,i+1)}$ peaks were observed only between the NH proton resonances of the Ser^7–Gln^8 and Arg^8–His^{10}. Moreover, strong sequential $d_{\alpha N(i,i+1)}$ peaks were detected along the C terminal region, from Pro^6 to Gly^{11}. In all three analogues, absence of any long-range NOEs was observed which indicated the presence of a significant number of populations being adopted

Table 3 Observed inter-residue cross-peaks in the NOESY spectra and their intensities for Ac-MBP_{1-11} [4A] in DMSO-d_6 at 298 K

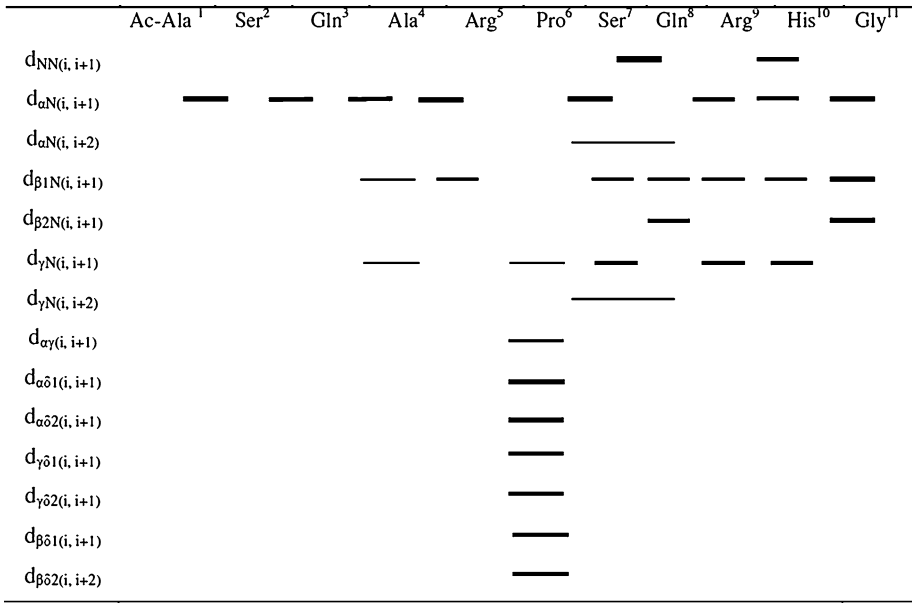

in the extended conformation. However, observation of a number of medium-range NOEs for different parts of the peptide backbone indicated the presence of populations with segments of local folded structure in the conformational ensemble.

Structural elucidation of Ac-MBP_{1-11}, Ac-MBP_{1-11}[4A] and Ac-MBP_{1-11}[4Y] analogues in solution

The MD simulation provided a wide range of conformations for the studied analogues. Among the 500 energy minimized conformations that were obtained after a 10 ns MD simulation, the most representative conformations were selected by examining their energy (time vs energy plots, data not shown), the energy convergence criterion root mean square deviation (RMSD force $\leq$ 0.001 kcal $mol^{-1}Å^{-1}$) and the results extracted from 2D H^1–H^1 TOCSY and NOESY spectra. More specifically, the adopted conformations were determined using the observed inter-residue cross-peaks of the NOESY spectra and their relative intensities which can be translated as distances between amino acid hydrogen atoms from each analogue. Dihedral angles [$\varphi_{(i+1)}$, $\psi_{(i+1)}$, $\varphi_{(i+2)}$, $\psi_{(i+2)}$] of the characteristic turns (results from NMR experiments) were used in order to identify the most representative conformations of the studied analogues.

Side chains present a slightly different topology in the bound state, however, this is expected as it is known that flexible molecules can be deformed upon binding to proteins [24]. Therefore, this methodology can be considered a robust method for identifying putative bioactive conformations. Theoretical methods arise as a solution for exploration of conformational space in the vicinity of conformers deduced from spectroscopic data and offer starting conformations for the conformational studies at the MHC binding site. Using the criteria described above (NMR and MD results), the representative conformations for Ac-MBP_{1-11}, Ac-MBP_{1-11}[4A] and Ac-MBP_{1-11}[4Y] are indicated in Figs. 2, 3, and 4.

The overall behavior along the trajectory of Ac-MBP_{1-11}, Ac-MBP_{1-11}[4A] and Ac-MBP1–11[4Y] for the MD run was analyzed. The following analysis focused on the ten (10) energy minimized conformations with the lowest energies that satisfy a set of criteria: (a) all backbone φ and ψ dihedral angles should occupy the allowed regions of the Ramachandran plot and (b) all backbone ω dihedrals should be *trans*. Particular attention was given to explore the flexibility of the side chains [25]. It is interesting to note that the central part of the peptide was almost similar in all conformations, whilst the N- and C- termini present flexible molecular segments. Generally, all conformations presented common features that could be summarized as: (1) low flexibility in the central part, (2) backbone extended structures and (3) it seems that each of these conformations could approach and bind to the MHC without any significant energy changes. The backbone overlapping (P1–P8 segment) energy favored final conformations (colored blue) for each analogue in comparison with the one (colored red) obtained from the crystal structure are presented in Figs. 2, 3, and 4. It is evident that there is no drastic differentiation of the backbone orientation for the analogues when they are compared with the one from the crystal structure.

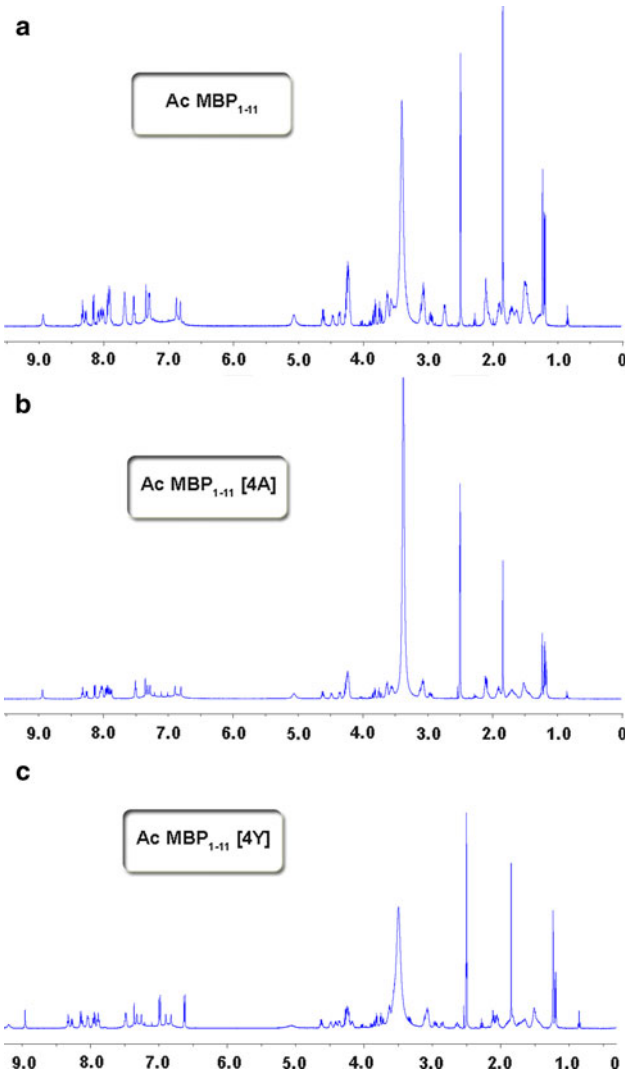

Fig. 1 ^{1}H NMR spectrum of Ac-$MBP_{1–11}$ (**a**), Ac-$MBP_{1–11}$[4A] (**b**) and Ac-$MBP_{1–11}$[4Y] (**c**) analogues in DMSO-d_6 recorded on a Bruker AVANCE 400 MHz spectrometer

Interaction of $MBP_{1–8}$[4A], $MBP_{1–8}$ and $MBP_{1–8}$[4Y] analogues with I–A^u

The final conformations of the studied analogues in complex with I–A^u were further analyzed in order to determine the hydrogen bond interactions between the peptide and the MHC molecule. The orientation of the primary TCR contacts was explored in order to correlate the conformation of the $MBP_{1–11}$ analogues with their EAE biological activity.

The crystal structure of the I–A^u- $MBP_{1–8}$[4Y] (PDB code: 1K2D) [12] complex was used as template for the MD simulations. After the MD simulations of $MBP_{1–8}$[4A] and $MBP_{1–8}$ with I–A^u, the peptides were isolated from the complexes and superimposed using also the conformation obtained from the X-ray structure. Figure 5 shows the superimposition of the Ca backbone atoms of the final peptide conformation of $MBP_{1–8}$[4A] with $MBP_{1–8}$ (RMSD of 1.12Å), $MBP_{1–8}$[4A] with $MBP_{1–8}$[4Y] (RMSD of 1.49Å) and $MBP_{1–8}$[4Y] with $MBP_{1–8}$ (RMSD of 1.41Å).

The side chain of the amino acid at position 4 (Ala, Tyr, Lys, respectively) was observed to have a different orientation for analogues $MBP_{1–8}$[4A] and $MBP_{1–8}$[4Y] compared to the native $MBP_{1–8}$ peptide whilst the Cα atom of Lys and Tyr is in good agreement (Fig. 5). The other significant MHC contacts Ser^2, Ser^7 and Pro^6 seem to have the same orientation in the native and mutated analogues. It is clear that no major conformational change occurred. In the $MBP_{1–8}$[4A] analogue, the Gln^3, Arg^5 and Pro^6 residues, which are complexed with TCR, are no longer prominent and solvent exposed, and hence are not available for interaction with the TCR (Fig. 6). On the other hand, the amino acid at position 4, which serves a major MHC binding residue, remained buried in the P6 pocket of I–A^u for the analogues $MBP_{1–8}$[4Y] and $MBP_{1–8}$ but not for $MBP_{1–8}$[4A] (Fig. 6, 7). Moreover, the intramolecular hydrogen bonds between the Gln^3 and Arg^5 (Fig. 7) for the $MBP_{1–8}$ and $MBP_{1–8}$[4Y] peptides were absent in the $MBP_{1–8}$[4A] analogue. The absence of these intramolecular hydrogen bonds in $MBP_{1–8}$[4A] peptide, with Ala at position 4, gives freedom to the side chain amide group of Gln^3 and allows it to approach and become buried within the I–A^u molecule. It's interface effectively prevents clear solvent exposure of the TCR contact (Gln^3) in the $MBP_{1–8}$[4A] analogue. This finding is in agreement with studies showing that the $AcMBP_{1–11}$[4A] analogue does not induce EAE but instead inhibits the development of EAE symptoms when co-injected with the immunodominant $AcMBP_{1–11}$. These results not only suggest differentiation of the binding affinity with I–A^u but also changes to the orientation of primary TCR contact residue and provide insight into the EAE profile of the peptides studied. In a previous study of ours, the different orientation of His^{88} and Phe^{89} (TCR contact) in the [Arg^{91}, Ala^{96}]$MBP_{87–99}$ and [$Ala^{91,96}$]$MBP_{87–99}$ analogues of the immunodominant $MBP_{87–99}$ epitope explained the in vivo EAE antagonistic activity of these analogues [20, 26–30].

The hydrogen bond interactions between peptide analogues in complex with I–A^u (pdb code 1K2D) [12] are depicted in Table 4 and Fig. 7. $MBP_{1–8}$[4Y]/I–A^u complex formed 7 H-bond contacts compared to $MBP_{1–8}$/I–A^u (5 H-bond contacts) and $MBP_{1–8}$[4A]/I–A^u (7 H-bond contacts) after the MD simulation. Noteworthy is the lack of H-bond involvement of peptide residue P1 (Ala^1) with any residue in the near vicinity of the peptide or MHC. The salt bridge found in the 1K2D crystal structure [12] ($MBP_{1–8}$[4Y]/I–A^u) between Arg^{P5} and $Glu^{74\beta}$ was conserved for the molecular models of $MBP_{1–8}$[4A] and $MBP_{1–8}$ in complex with I–A^u.

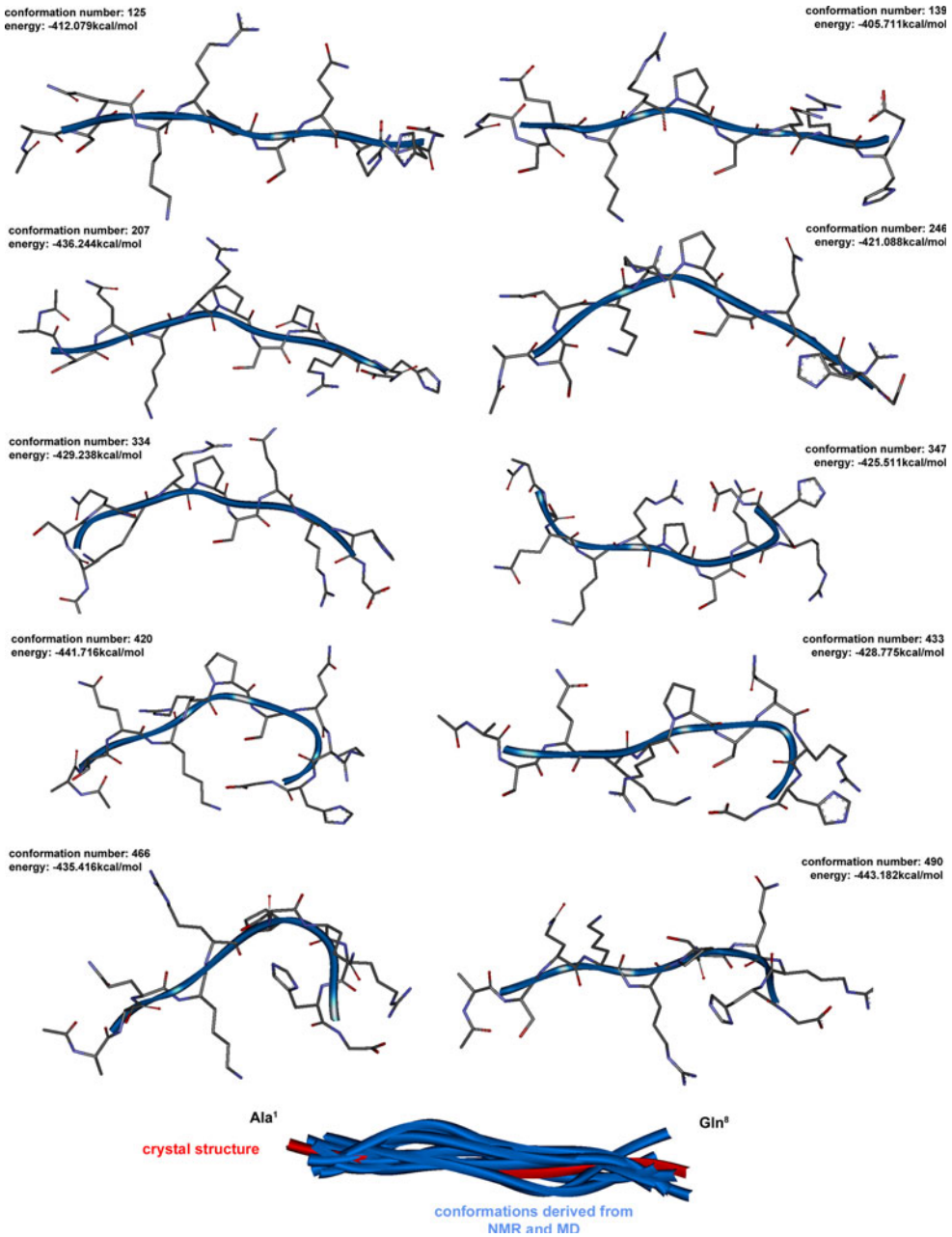

Fig. 2 The ensemble of conformers generated after applying molecular dynamics simulations and energy minimization to the Ac-MBP_{1-11} analogue

Conclusions

Molecular dynamics calculations in combination with NMR structure determination were employed to explore the conformational space for MBP_{1-11} analogues that fulfill the experimental distance restraints. In the present study, both approaches were evaluated in an attempt to generate as many distinct conformational populations in solution as possible. Indeed, a bundle of conformers that were in accordance with the most critical NOEs were obtained, representing the true flexibility of the peptide. In particular, the molecule appeared to have a flexible termini and restricted central motion. Interaction of the side chains that are largely populated in the conformational ensemble are present, demonstrating that NMR complements by MD are valuable tools for the proposal of bioactive conformations. The MBP_{1-8}[4Y]/I–A^u crystal structure was used to study the binding of the linear peptides MBP_{1-8} and MBP_{1-8}[4A] in order to derive conclusions regarding the biological activity of the acetylated MBP_{1-11} analogues. It was found that the main MHC contact residues (Ser^2, Pro^6 and Ser^7) remained in the same position for all peptides. However, Gln^3 (TCR contact) was not solvent exposed so as to interact with TCR for the antagonist MBP_{1-8}[4A] peptide. Knowledge of the relationship of peptide conformation and bioactivity will facilitate the rational design and synthesis

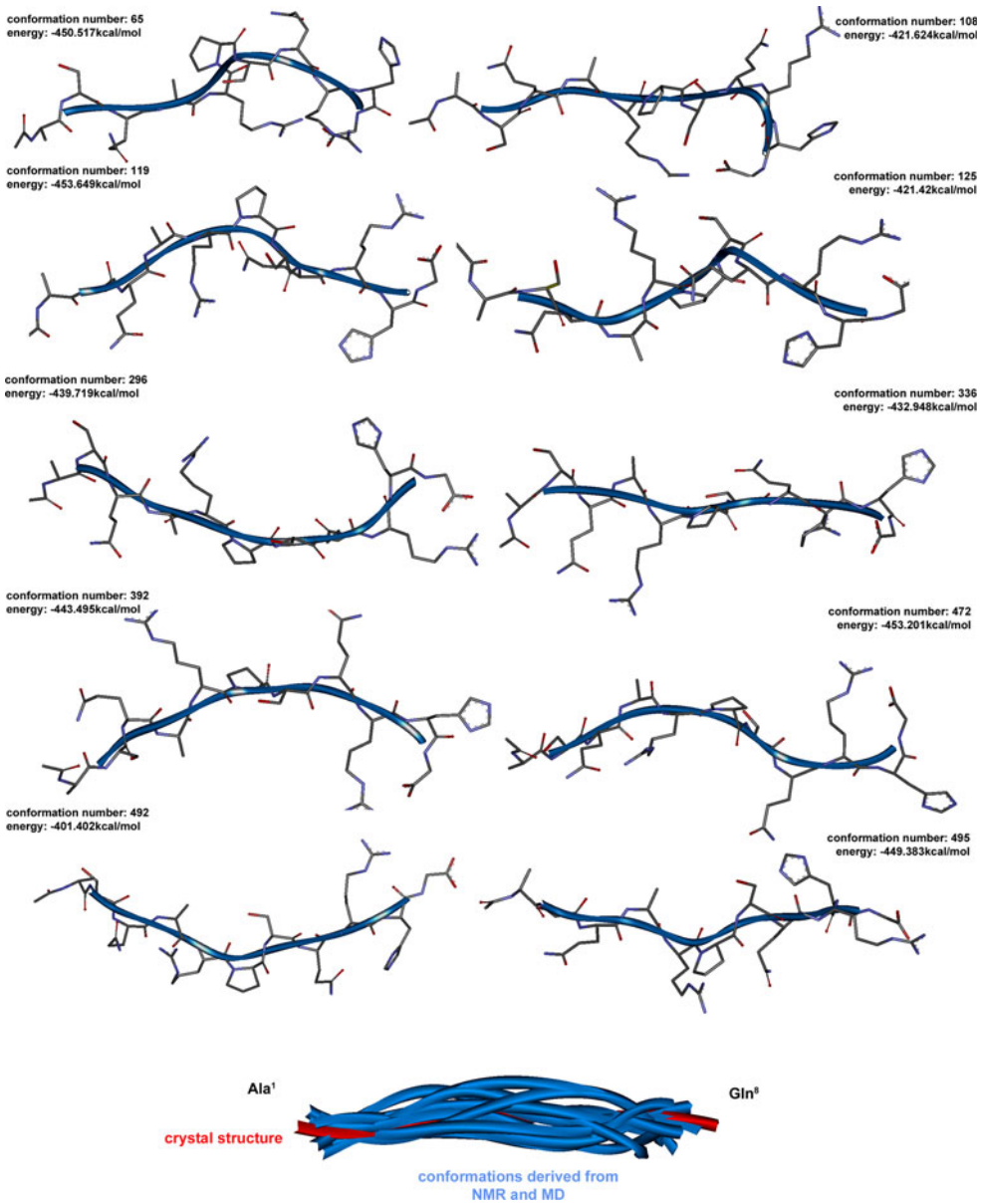

Fig. 3 The ensemble of conformers generated after applying molecular dynamics simulations and energy minimization to the Ac-MBP$_{1-11}$[4A] analogue

of novel peptide analogues and ultimately peptide mimetic molecules for the immunotherapy of MS.

Experimental section

Synthetic procedure

2-Chlorotrityl chloride resin (0.7–1.0 mmol Cl^-/g resin, 200–400 mesh), Fmoc-Gly-OH, Fmoc-His(Trt)-OH, Fmoc-Arg(Pbf)-OH, Fmoc-Gln-OH, Fmoc-Ser(tBu)-OH, Fmoc-Pro-OH, Fmoc-Lys(Mtt)-OH, Fmoc-Ala-OH and Fmoc-Tyr-OH were obtained from Chemical and Biopharmaceutical Laboratories of Patras, Patras, Greece. All solvents and other reagents were purchased from Merck, Sigma-Aldrich and Fluka chemical companies. DC-Alufolien Kieselgel 60 (Merck) was used for Thin Layer Chromatography (TLC) analysis of synthetic products with the following eluent solvent: *n*-butanol/acetic acid/water (BAW) 4:1:1 (v/v/v). Peptides were purified by semi-preparative reverse phase high performance liquid chromatography (RP-HPLC) on a Waters system equipped with a 600E controller and a Waters 996 photodiode array UV detector. The analysis was controlled by an operating Millenium 2.1 system and a Nucleosil C-18 reversed phase analytical column (250 × 10 mm with 7 μm packing material). Electron spray ionization mass spectroscopy (ESI–MS) experiments were performed on a TSQ 7000

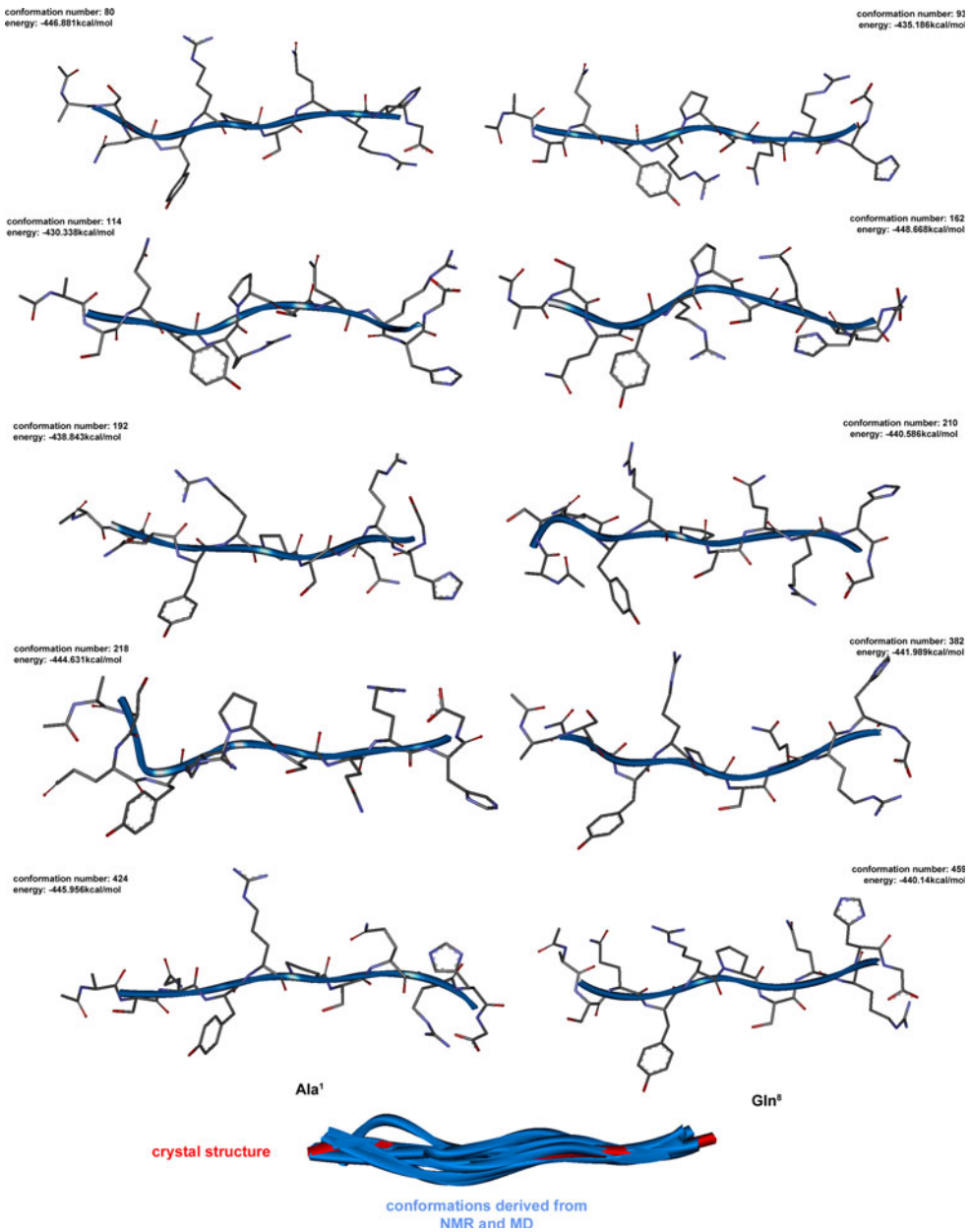

Fig. 4 The ensemble of conformers generated after applying molecular dynamics simulations and energy minimization to the Ac-MBP_{1-11}[4Y] analogue

spectrometer (Electrospray Platform LC of Micromass) coupled to a MassLynx NT 2.3 data system.

Synthesis of Ac-MBP_{1-11}, Ac-MBP_{1-11}[4A] and Ac-MBP_{1-11}[4Y] analogues

The linear peptides were prepared on 2-chlorotrityl chloride resin (CLTR-Cl) using the Fmoc/tBu solid-phase peptide synthetic method [31–35]. The first N^{α} Fmoc (9-fluorenylmethyloxycarboxyl)-protected amino acid Fmoc-Gly-OH was coupled (esterified) to the resin in the presence of diisopropylethylamine (DIPEA) (4.5 equiv, 0.75 mL) in dichloromethane (DCM) in 1 h at RT. A mixture of DCM/MeOH/DIPEA (85:10:5, 7 mL) was then added and the mixture was stirred for another 10 min at RT. The Fmoc-Gly-resin was subsequently filtered and washed with DCM (3 × 10 mL), 2-propanol (iPrOH) (2 × 10 mL) and *n*-hexane (2 × 10 mL) and dried under vacuum for 24 h.

The remaining protected peptide chains were assembled by sequential couplings of the appropriate Fmoc protected amino acids (2.5 equiv), in the presence of *N,N′*-diisopropylcarbodiimide (DIC) (2.75 equiv) and 1-hydroxybenzotriazole (HOBt) (3.75 equiv) in *N,N*-dimethylformamide (DMF) for 4–6 h. The following Fmoc protected amino acids were used for the synthesis: Fmoc-His(Trt)-OH, Fmoc-Arg(Pbf)-OH, Fmoc-Gln-OH, Fmoc-Ser(tBu)-OH, Fmoc-Pro-OH, Fmoc-Arg(Pbf)-OH, Fmoc-Lys(Mtt)-OH or

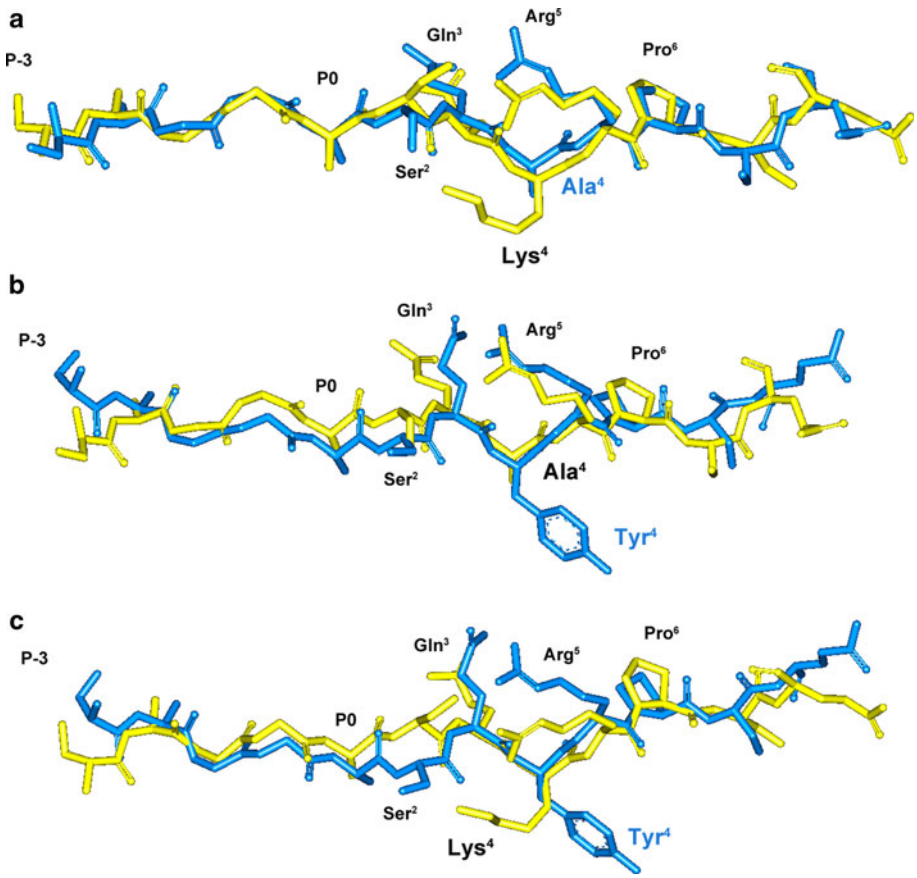

Fig. 5 Overlay of **a** $MBP_{1–8}$ with the $MBP_{1–8}$[4A], **b** $MBP_{1–8}$[4Y] (1K2D pdb code) with the $MBP_{1–8}$[4A] and **c** $MBP_{1–8}$ with the $MBP_{1–8}$[4Y] (1K2D pdb code). The side chain of the amino acid at position 4 (Ala, Tyr, Lys, respectively) has a different orientation in $MBP_{1–8}$[4A] and $MBP_{1–8}$[4Y] analogues compared to $MBP_{1–8}$ peptide whilst the Cα atom of Lys and Tyr is in good matching. The MHC contacts Ser^2, Ser^7 and Pro^6 have the same orientation in native and mutated analogues

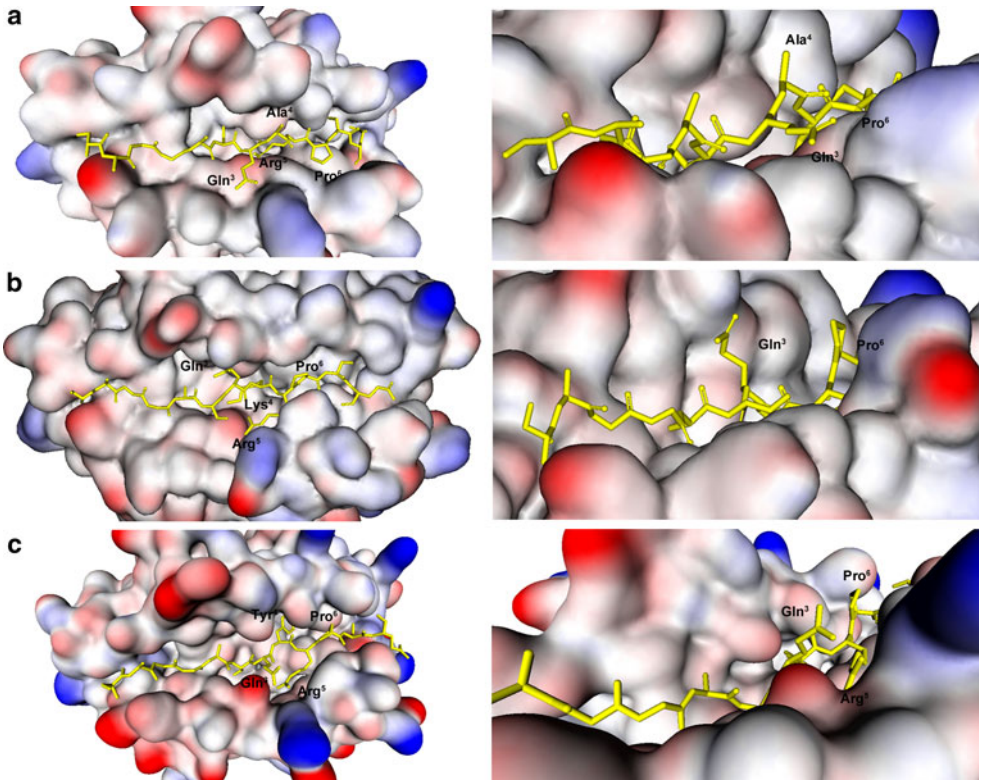

Fig. 6 Location of the peptide analogues $MBP_{1–8}$[4A] (**a**), $MBP_{1–8}$ (**b**) and $MBP_{1–8}$[4Y] (**c**) within the $I–A^u$ binding groove. The MHC is shown as molecular surface whereas the peptides are shown as *yellow* stick. The TCR contact residues (Gln^3 and Pro^6) have a different orientation in $MBP_{1–8}$[4A]/$I–A^u$ complex compared to $MBP_{1–8}$/$I–A^u$ $MBP_{1–8}$[4Y]/$I–A^u$. They are not solvent exposed and available to interact with the TCR receptor

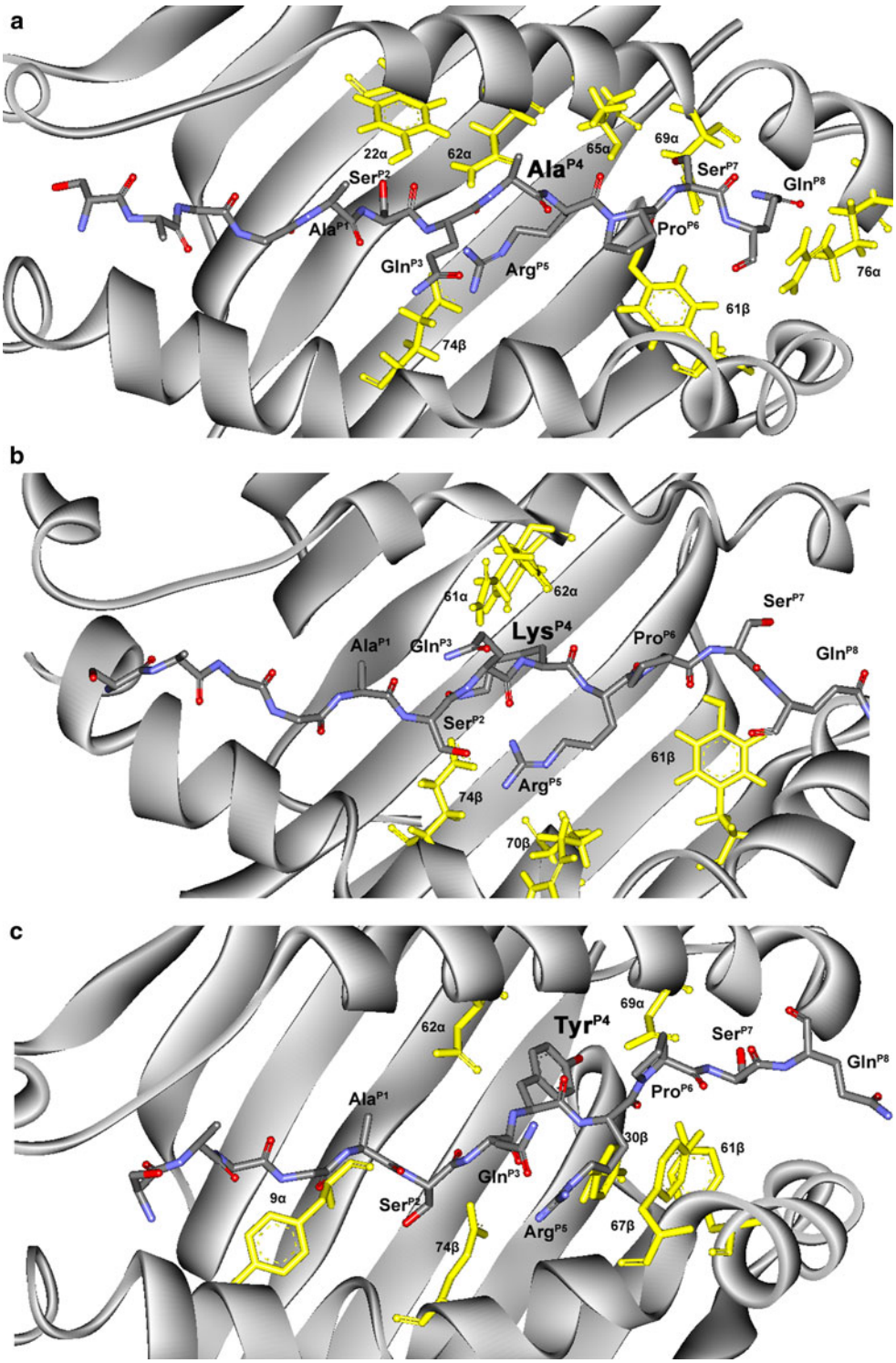

Fig. 7 The interacting residues between I–A^{u} and MBP$_{1–8}$[4A] (**a**), MBP$_{1–8}$ (**b**), MBP$_{1–8}$[4Y] (**c**) are shown. The important residues of the α and β chains of I–A^{u} for interaction with the peptides are indicated in *yellow*. P1–P8 residues are in *bold black font*

Fmoc-Ala-OH or Fmoc-Tyr-OH, Fmoc-Gln-OH, Fmoc-Ser(tBu)-OH and Fmoc-Ala-OH (Scheme 1). The completeness of each coupling was verified by the Kaiser test and TLC using a BAW, 4:1:1 (v/v/v) eluent system and the Fmoc protecting group was removed by treatment with piperidine solution (20% in DMF, 2 × 20 min). The acetylation of N$^{\alpha}$ terminal was achieved on the resin with acetic anydride/DIPEA in DMF for 1 h at RT. The synthesized protected peptide on the resin was then cleaved with the splitting solution dichloromethane/2,2,2-trifluoroethanol/acetic acid (DCM/TFE/AcOH, 7/2/1, 2 h at RT). The mixtures were filtered, solvents were removed on a rotary evaporator and the obtained oily products were precipitated from cold dry diethyl ether as amorphous

Table 4 Hydrogen bond interactions between MBP_{1-8}[4A], MBP_{1-8} and MBP_{1-8}[4Y] peptide side chains and $I–A^u$

Peptide residue	MBP_{1-8}[4A]/$I–A^u$	MBP_{1-8}/$I–A^u$	MBP_{1-8}[4Y]/$I–A^u$
Ala^{P1}	–	–	–
Ser^{P2}	$Tyr^{22\alpha}$	–	$Tyr^{9\alpha}$
Gln^{P3}	$Asn^{62\alpha}$, $Glu^{74\beta}$	$Gln^{61\alpha}$	–
$Lys/Tyr/Ala^{P4}$	$Asn^{62\alpha}$	$Asn^{62\alpha}$, $Glu^{74\beta}$	$Asn^{62\alpha}$
Arg^{P5}	$Glu^{74\beta}$	$Glu^{74\beta}$, $Arg^{70\beta}$	$Tyr^{30\beta}$, $Tyr^{61\beta}$, $Glu^{74\beta}$
Pro^{P6}	$Tyr^{61\beta}$, $Thr^{65\alpha}$	$Tyr^{61\beta}$	$Tyr^{67\beta}$
Ser^{P7}	$Asn^{69\alpha}$	–	$Asn^{69\alpha}$
Gln^{P8}	$Arg^{76\alpha}$	–	–

white solids. The dried linear protected peptides were treated with 65% TFA in DCM in the presence of 10% 1, 2-ethanedithiol and anisole as scavengers for 5 h at room temperature. The solvents were removed on a rotary evaporator and the obtained oily products were precipitated from cold dry diethyl ether as amorphous light–yellow solids (Scheme 1). The purification was carried out using semi-preparative RP-HPLC and peptide purity was assessed by analytical RP-HPLC (column: Nucleosil C18, 5 μm, 4.6 × 250 mm) and were identified by ESI–MS.

Nuclear magnetic resonance spectroscopy (NMR)

NMR spectra were recorded on a Bruker AVANCE 500 MHz spectrometer at 298 K, using DMSO-d_6 as solvent. The concentration of the samples was 9 mg/0.6 mL, approximately. Routine parameters were used recording the ^1H spectra. The sweep width was 6,000 Hz and the chemical shifts are reported with respect to the resonance of the solvent in DMSO-d_6 solution, which was used as the internal standard. All 2D spectra were acquired using TPPI

Scheme 1 Synthetic procedure for Ac-MBP_{1-11}, Ac-MBP_{1-11}[4A] and Ac-MBP_{1-11}[4Y] peptide analogues

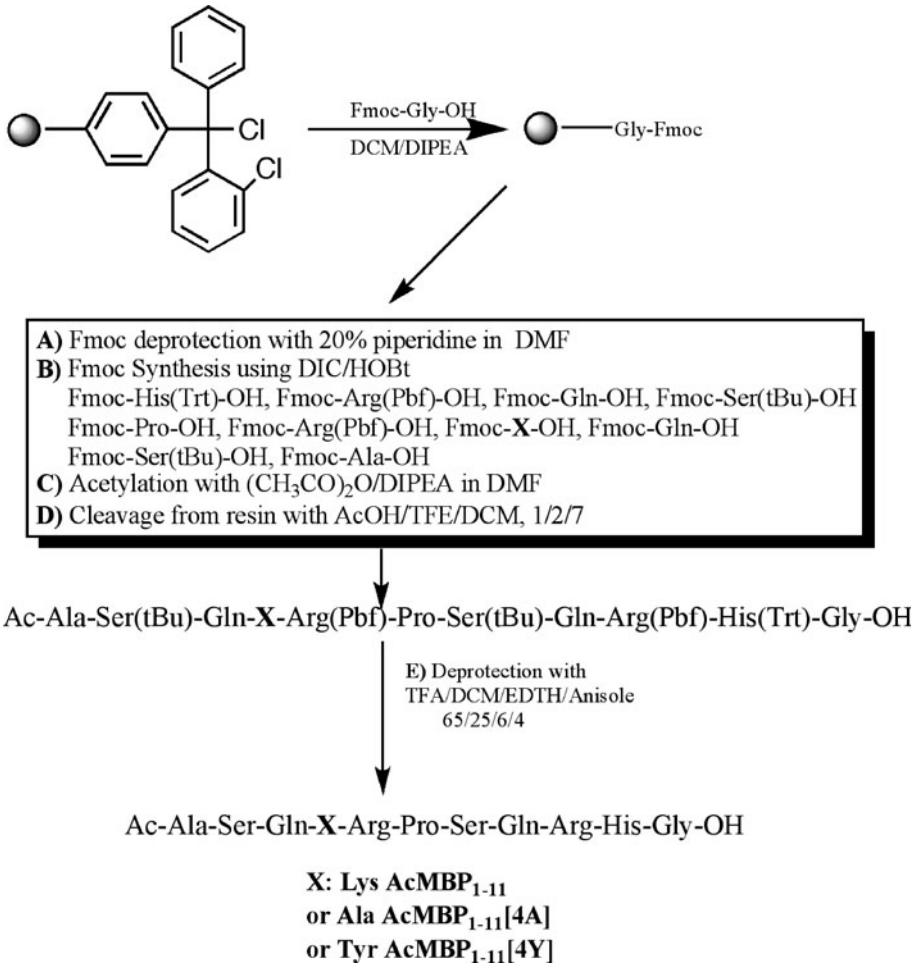

method for quadrature detection. The 2D measurements were recorded using 512 increments of 2 K complex data points and 80 scans per increment for 2D ^{1}H NOESY and 16 scans for 2D ^{1}H TOCSY experiments, respectively. The mixing time for NOESY spectra was 350 ms, and that for TOCSY was 90 ms. Data were processed using the TopSpin standard software. The t_1 dimension was zero-filled to 1 K real data points, and 60° phase-shifted square sine bell window functions were applied in both dimensions.

Theoretical calculations

Molecular modeling

Computer calculations were performed on a Pentium IV 2.14 GHz workstation using Discovery Studio v2.0 by Accelrys Software Inc., [36]. Molecular dynamics simulations were performed and the derived conformations were examined for consistency with experimental distance and dihedral information derived from the obtained NOEs. Thus, populations of various conformers that represent local minima at the potential energy surface were identified.

Generating the starting conformation

The starting conformations of Ac-MBP_{1-11}[4A], Ac-MBP_{1-11}[4K] and Ac-MBP_{1-11}[4Y] were extendedly built, consisting of L-amino acids, using the CHARMm force field [37]. The studies were performed using DMSO (dielectric constant 45) [20, 26, 27] as solvent, in agreement with the NMR experiments. The implicit solvent model Generalized Born [38, 39] was used, as well as the SHAKE algorithm which serves to satisfy bond geometry constraints during the molecular dynamics simulations. The structures were then minimized using a succession of three methods: steepest descents (SD) to remove unfavorable steric contacts, then conjugate gradient (CG) to find its local minimum, followed by truncated Newton (TN). TN is the most efficient large scale non-linear optimization algorithm known. In all cases, energy convergence criterion was the root mean square deviation (RMSD) $\leq$ 0.001 Å.

Molecular dynamics studies

One set of unrestrained Molecular Dynamics simulations was performed using the CHARMm force field as follows: Heating from 0 to 300 K gradually and equilibration were set with a time step of 0.001 ps for a total time of 3 ns while the time step of Production was 0.001 ps for a total time of 10 ns. Parameters on saving results frequencies were set in such a way in order to extract 500 conformations for each molecule. These structures were minimized with a 500 step conjugate gradient algorithm and RMSD 0.001 Å as the energy convergence criterion. Ten (10) conformations were selected according to their energy and NMR data. The selected structures had backbone dihedral angles φ and ψ within the core region of the Ramachandran map [40, 41] and *trans* ω dihedral angles [42].

Molecular dynamics of ASQXRPSQ segment of MBP_{1-8}[4Y], MBP_{1-8}[4A] and MBP_{1-8} analogues in complex with I–A^{u}

The models of MBP_{1-8} and MBP_{1-8}[4A] peptide analogues in complex with MHC class II molecule I–A^{u} were based on the crystal structure of I–A^{u} complexed to N-terminal MBP peptide with Tyrosine (Y) at position 4 (P-3 P-2 P-1 P0 ASQ**Y**RPSQ, 1K2D) The crystal structure includes the leader sequence (SRGG) as described in He et al. [12]. (residues P-3–P0) and only the first eight amino acids of the MBP_{1-11} epitope (ASQ**Y**RPSQRHG; residues P1–P8 underlined). The simulation studies were carried out in the first eight amino acids of the MBP_{1-11} epitope and conserving the leader sequence from crystal model whilst the residue P4 (Y) was replaced to either alanine (A) or lysine (K). Computer calculations were performed on a Pentium IV workstation using MOE2008.10 by Chemical Computing Inc [43] on LINUX interface and the CHARMm force field was employed for the energy minimizations and molecular dynamics simulations. Prior to the molecular dynamics simulation, structures were relaxed using the SD algorithm until the RMSD was less than 0.1 kcal mol^{-1}, then CG and finally Truncated Newton until the RMSD was <0.01 the kcal mol^{-1}. A distance dependent dielectric was used to simulate aqueous solvent conditions. Peptide molecules and all atoms within a 10 Å radius of the peptide were subsequently heated to room temperature (300 K) for 0.5 ns and equilibrated at this temperature for a further 0.1 ns before commencing the molecular dynamics run for 5 ns, storing the structure every 10 ps.

The final conformation was selected for all further analysis. The RMSD between the backbone Cα atoms was calculated for all residues between MBP_{1-8}, MBP_{1-8}[4A] and MBP_{1-8}[4Y] as a measure of variation in peptide conformation. All satisfied H-bonds and salt bridges between peptide and I–A^{u} were identified. Residues from the peptide are labeled with the superscripts P-3–P8 while those from the I–A^{u} molecules with the simple numerical superscripts and α/β superscript for the respective chain.

Acknowledgments D. Laimou was supported by the University of Patras (Grant K. Karatheodoris). M. Katsara was supported by the Ministry of Development Secretariat of Research and Technology of Greece (Grant Aus. 005) and Du Pré grant from MSIF. V. Apostolopoulos and E. Lazoura were in part supported by an NH&MRC project grant 223310. In addition, V. Apostolopoulos was supported

by NH&MRC of Australia R. Douglas Wright Fellowship (223316). E. Lazoura, M. Katsara and V. Apostolopoulos were located at the Austin Research Institute when the studies were undertaken prior to the merger with the Burnet Institute. Hence, E. L, M. K and V. A. would like to acknowledge the support of the Austin Research Institute.

References

1. Steinman L (1996) Multiple sclerosis: a coordinated immunological attack against myelin in the central nervous system. Cell 85:299–302
2. Martin R, McFarland H, McFarlin D (1992) Immunological aspects of demyelinating diseases. Annu Rev Immunol 10:153–187
3. Hemmer B, Archelos JJ, Hartung HP (2002) New concepts in the immunopathogenesis of multiple sclerosis. Nat Rev Neurosci 3:291–301
4. Hafler DA, Slavik JM, Anderson DE, O'Connor KC, De Jager P, Baecher-Allan C (2005) Multiple sclerosis. Immunol Rev 204: 208–231
5. Zamvil SS, Steinman L (1990) The T lymphocyte in experimental allergic encephalomyelitis. Ann Rev Immunol 8:579–621
6. Zamvil SS, Mitchell DJ, Moore AC, Schwarz AJ, Stiefel W, Nelson PA, Rothbard JB, Steinman L (1987) T-cell specificity for class II(I–A) and the encephalitogenic N-terminal epitope of the autoantigen myelin basic protein. J Immunol 139:1075–1079
7. Zamvil SS, Mitchell DJ, Moore AC, Kitamura K, Steinman L, Rothbard JB (1986) T-cell epitope of the autoantigen myelin basic protein that induces encephalomyelitis. Nature 324:258–260
8. Gautam AM, Pearson CI, Smilek DE, Steinman L, McDevitt HO (1992) A polyalanine peptide with only five native myelin basic protein residues induces autoimmune encephalomyelitis. J Exp Med 176:605–609
9. Wraith DC, Smilek DE, Mitchell DJ, Steinman L, McDevitt HO (1989) Antigen recognition in autoimmune encephalomyelitis and the potential for peptide-mediated immunotherapy. Cell 59:247–255
10. Anderton SM, Radu CG, Lowrey PA, Ward ES, Wraith DC (2001) Negative selection during the peripheral immune response to antigen. J Exp Med 193:1–11
11. Lee C, Liang MN, Tate KM, Rabinowitz JD, Beeson C, Jones PP, McConnell HM (1998) Evidence that the autoimmune antigen myelin basic protein (MBP) Ac1–9 binds towards one end of the major histocompatibility complex (MHC) cleft. J Exp Med 187: 1505–1516
12. He XL, Radu C, Sidney J, Sette A, Ward ES, Garcia KC (2002) Structural snapshot of aberrant antigen presentation linked to autoimmunity: the immunodominant epitope of MBP complexed with I–A^u. Immunity 17:83–94
13. Fugger L, Liang J, Gautam A, Rothbard JB, McDevitt HO (1996) Quantitative analysis of peptides from myelin basic protein binding to the MHC class II protein, I-Au, which confers susceptibility to experimental allergic encephalomyelitis. Mol Med 2:181–188
14. Metzler B, Wraith DC (1993) Inhibition of experimental autoimmune encephalomyelitis by inhalation but not oral administration of the encephalitogenic peptide: influence of MHC binding affinity. Int Immunol 5:1159–1165
15. Mason K, Denney DW, McConnell HM (1995) Myelin basic protein peptide complexes with the class II MHC molecules I–A^u and I–A^k form and dissociate rapidly at neutral pH. J Immunol 154:5216–5227
16. Fairchild PJ, Wildgoose R, Atherton E, Webb S, Wraith DC (1993) An autoantigenic T cell epitope forms unstable complexes with class II MHC: a novel route for escape from tolerance induction. Intern Immunol 5:1151–1158
17. Goverman J, Woods A, Larson L, Weiner LP, Hood L, Zaller DM (1993) Transgenic mice that express a myelin basic protein-specific T cell receptor develop spontaneous autoimmunity. Cell 72:551–560
18. Maynard J, Petersson K, Wilson DH, Adams EJ, Blondelle SE, Boulanger MJ, Wilson DB, Garcia KC (2005) Structure of an autoimmune T cell receptor complexed with class II peptide-MHC: insights into MHC bias and antigen specificity. Immunity 22:81–92
19. Morikis D, Roy M, Sahu A, Troganis A, Jennings PA, Tsokos GC, Lambris JD (2002) The structural basis of compstatin activity examined by structure-function-based design of peptide analogs and NMR. J Biol Chem 277:14942–14953
20. Mantzourani ED, Blokar K, Tselios TV, Matsoukas JM, Platts JA, Mavromoustakos TM, Grdadolnik SG (2008) A combined NMR and molecular dynamics simulation study to determine the conformational properties of agonists and antagonists against experimental autoimmune encephalomyelitis. Bioorg Med Chem 16:2171–2182
21. Laimou DK, Katsara M, Matsoukas MI, Apostolopoulos V, Troganis AN, Tselios TV (2010) Structural elucidation of Leuprolide and its analogues in solution: insight into their bioactive conformation. Amino Acids 39(5):1147–1160
22. Dyson HJ, Wright PE (1991) Defining solution conformations of small linear peptides. Annu Rev Biophys Biophys Chem 20: 519–538
23. Wright PE, Dyson HJ, Lerner RA (1988) Conformation of peptide fragments of proteins in aqueous solution: implications for initiation of protein folding. Biochemistry 27:7167–7175
24. Nicklaus MC, Wang S, Driscoll JS, Milne GW (1995) Conformational changes of small molecules binding to proteins. Bioorg Med Chem 3:411–428
25. Galzitskaya O, Caflisch A (1999) Solution conformation of phakellistatin 8 investigated by molecular dynamics simulations. J Mol Graph Modell 17:19–27
26. Mantzourani ED, Platts JA, Brancale A, Mavromoustakos TM, Tselios TV (2007) Molecular dynamics at the receptor level of immunodominant myelin basic protein epitope 87–99 implicated in multiple sclerosis and its antagonists altered peptide ligands: triggering of immune response. J Mol Graph Modell 26:471–481
27. Mantzouran ED, Tselios TV, Grdadolnik SG, Platts JA, Brancale A, Deraos G, Matsoukas JM, Mavromoustakos TM (2006) Comparison of proposed putative active conformations of myelin basic protein epitope 87–99 linear altered peptide ligands by spectroscopic and modeling studies: the role of positions 91 and 96 in T-cell receptor activation. J Med Chem 49:6683–6691
28. Mantzourani ED, Mavromoustakos TM, Platts JA, Matsoukas JM, Tselios TV (2005) Structural requirements for binding of myelin basic protein (MBP) peptides to MHC II: effects on immune regulation. Curr Med Chem 12(13):1521–1535
29. Aldulaijan S, Platts JA (2010) Theoretical prediction of a peptide binding to major histocompatibility complex II. J Mol Graph Model 29(2):240–245
30. Mantzourani E, Laimou D, Matsoukas M-T, Tselios T (2008) Peptides as therapeutic agents or drug leads for autoimmune, hormone dependent, cardiovascular diseases. Anti-inflam Anti-all Agents 7(4):294–306
31. Tselios T, Probert L, Daliani I, Matsoukas E, Troganis A, Gerothanassis IP, Mavromoustakos T, Moore GJ, Matsoukas JM (1999) Design and synthesis of a potent cyclic analogue of the myelin basic protein epitope MBP72–85: importance of the Ala81 carboxyl group and of a cyclic conformation for induction of experimental allergic encephalomyelitis. J Med Chem 42(7):1170–1177

32. Tselios T, Daliani I, Probert L, Deraos S, Matsoukas E, Roy S, Pires J, Moore G, Matsoukas JM (2000) Treatment of experimental allergic encephalomyelitis (EAE) induced by guinea pig myelin basic protein epitope 72–85 with a human MBP(87–99) analogue and effects of cyclic peptides. J Bioor Med Chem 8:1903–1909
33. Tselios T, Daliani I, Deraos S, Thymianou S, Matsoukas E, Troganis A, Gerothanassis I, Mouzaki A, Mavromoustakos T, Probert L, Matsoukas J (2000) Treatment of experimental allergic encephalomyelitis (EAE) by a rationally designed cyclic analogue of myelin basic protein (MBP) epitope 72–85. J Bioor Med Chem Let 10:2713–2717
34. Matsoukas J, Apostolopoulos V, Kalbacher H, Papini AM, Tselios T, Chatzantoni K, Biagioli T, Lolli F, Deraos S, Papathanassopoulos P, Troganis A, Mantzourani E, Mavromoustakos T, Mouzaki A (2005) Design and synthesis of a novel potent myelin basic protein epitope 87–99 cyclic analogue: enhanced stability and biological properties of mimics render them a potentially new class of immunomodulators. J Med Chem 48:1470–1480
35. Barlos K, Gatos D, Schafer W (1991) Synthesis of prothymosin α(ProTα)—a protein consisting of 109 amino acid residues. Angew Chem Int Ed Engl 30(5):590–593
36. Discovery Studio v2.0 Molecular Modeling Systems, supplied by Accelrys Software (2005) Cerius^2 modeling environment, release 4.8. Accelrys Software, San Diego
37. Brooks BR, Bruccoleri RE, Olafson BD, States DJ, Swaminathan S, Karplus M (1983) CHARMM: a program for macromolecular energy, minimization, and dynamics calculations. J Comp Chem 4:187–217
38. Chen J, Wonpil I, Brooks CL (2006) Balancing solvation and intramolecular interactions: toward a consistent generalized born force field. J Am Chem Soc 128(11):3373–3728
39. Dominy B, Brooks CL (1999) Development of a generalized born model parameterization for proteins and nucleic acids. J Phys Chem 103:3765–3773
40. Ramachandran GN, Sasisekharan V (1968) Conformations of polypeptides and proteins. Adv Prot Chem 23:283–437
41. Ramakrishhan C, Ramachandran GN (1965) Stereochemical criteria for polypeptide and protein chain conformations. II. Allowed conformations for a pair of peptide units. Biophys J 5:909–933
42. Laskowski R, McArtur M, Moss D, Thornton J (1993) PROCHECK: a program to check the stereochemical quality of protein structures. J Appl Cryst 26:283–291
43. Chemical Computing Group Inc. 1010 Sherbrooke Street W, Suite 910; Montreal, QC, Canada H3A 2R7